Neurocomputing 354 (2019) 49–60

Contents lists available at ScienceDirect

Neurocomputing

journal homepage: www.elsevier.com/locate/neucom

Extending the hybrid methodology for orbit propagation by fitting techniques

Iván Pérez[a,*], Montserrat San-Martín[b], Rosario López[c], Eliseo P. Vergara[a], Alexander Wittig[d,e], Juan Félix San-Juan[c,*]

[a] Scientific Computing Group (GRUCACI), University of La Rioja, San José de Calasanz 31, 26004 Logroño, Spain
[b] Scientific Computing Group (GRUCACI), University of Granada, Santander 1, 52005 Melilla, Spain
[c] Scientific Computing Group (GRUCACI), University of La Rioja, Madre de Dios 53, 26006 Logroño, Spain
[d] Advanced Concepts Team, European Space Agency, Keplerlaan 1, NL-2200 AG Noordwijk, The Netherlands
[e] University of Southampton, SO17 1BJ Southampton, UK

ARTICLE INFO

Article history:
Received 14 November 2017
Revised 4 April 2018
Accepted 26 May 2018
Available online 18 April 2019

Keywords:
Artificial satellite theory
Orbit propagator
Hybrid propagation methodology
Time series forecasting
Holt-Winters
Generalized additive models

ABSTRACT

The hybrid methodology for orbit propagation is a technique that allows improving the accuracy of any propagator for predicting the future trajectory of a satellite or space-debris object in orbit around the Earth. It is based on modeling the error of the base propagator to be enhanced. Both statistical time-series forecasting methods and machine-learning techniques can be used for that purpose. The standard procedure for developing a hybrid orbit propagator requires some initial control data, that is, a set of precise ephemerides corresponding to either real observations or accurately computed pseudo-observations, from which to model the base-propagator error dynamics. It also needs tuning the time-series forecaster from those control data. We propose an improvement to the hybrid methodology for orbit propagation, based on fitting new hybrid propagators from others previously developed for nearby initial conditions, which avoids the need for both the control data and the tuning process, and achieves comparable results.

1. Introduction

Artificial satellites around the Earth provide some critical services upon which society is increasingly dependent, such as telecommunications, meteorological observation and weather forecasting, satellite navigation, monitoring of land and marine resources, scientific studies, security and defense. Nevertheless, during the last decades all those services have been becoming increasingly threatened by space debris. Space debris is composed of objects that remain out of control, many of which share the same orbits as operative satellites, or cross their trajectories at some moment.

In order to maintain satellite services active, satellite operators must insure that space debris does not interfere with the satellites they control. Nonetheless, active debris removal is not technically nor economically viable at the present time. The only feasible solution consists in observing every perceptible object through a network of both optical and radar sensors, with the aim of cataloging them and tracking their trajectories. The concept is very similar to that of a control tower that were in charge of tracking the approximately 1200 current operative satellites and the estimated 29000 objects larger than 10 cm, 23000 of which are regularly tracked and maintained in the US Space Surveillance Network catalog. The objective of Space Surveillance and Tracking (SST) programs, which are integrated into the wider scope of Space Situational Awareness (SSA), is to guarantee the safety of operative-satellite orbits by predicting, and therefore avoiding, possible collisions.

Orbit propagation is a key tool for achieving this objective because it allows determining the future trajectory of space objects. It is based on integrating the dynamical system that describes how different forces affect the movement of each object. The most important force is the gravitational attraction from an ideally spherical and homogeneous Earth model, which causes a simple keplerian orbit that is easy to be determined. Nevertheless, there are certain perturbing forces, mainly caused by the non-uniformity of the Earth gravitational field, the atmospheric drag, the solar radiation pressure, and the gravitational pull from both the Sun and

* Corresponding authors.
E-mail addresses: ivan.perez@unirioja.es (I. Pérez), momartin@ugr.es (M. San-Martín), rosario.lopez@unirioja.es (R. López), eliseo.vergara@unirioja.es (E.P. Vergara), alexander.wittig@esa.int, a.wittig@soton.ac.uk (A. Wittig), juanfelix.sanjuan@unirioja.es (J.F. San-Juan).

https://doi.org/10.1016/j.neucom.2018.05.138
0925-2312/

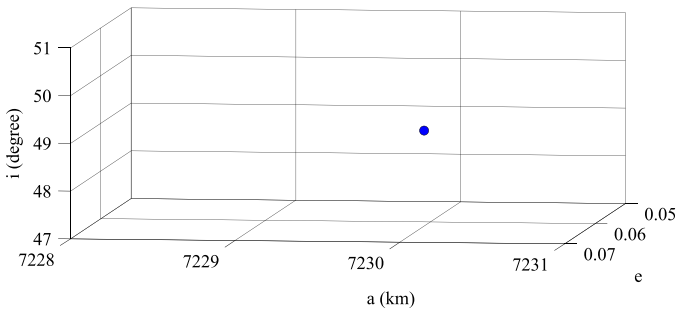

Fig. 1. Situation of the initial conditions of the illustrative satellite in the 3D [semi-major axis, eccentricity, inclination] domain.

the Moon, which modify the trajectory of the space object in orbit, converting its determination into a complex mathematical and computational problem.

Orbit propagators are not completely precise for different reasons. Sometimes the perturbation models they implement are much simpler than the physical phenomena they try to describe. Other times, the analytical approximations assumed during their development have a negative impact on their mid- and long-term accuracy.

Space Situational Awareness (SSA) has imposed new constraints on orbit propagation. As the density of space objects in orbit around the Earth keeps increasing, mainly because of the proliferation of space debris, there is a growing demand for agile and accurate methods for determining the future trajectory of cataloged objects. Traditionally, the long computational time of precise *numerical propagators* [1,2], or the limited accuracy of fast *analytical propagation theories* [3–7], depending on the context, had been tolerated. *Semi-analytical propagators* [8–10] allowed reaching a compromise between agility and precision. Nevertheless, current and future SSA necessities are demanding innovative approaches that allow overcoming the aforementioned disadvantages of conventional propagators.

In this context, the *hybrid methodology for orbit propagation* has been recently proposed [11–13]. It aims to enhance the precision of any orbit propagator by modeling its error with respect to *control data*, which consists of real observations or accurately computed pseudo-observations during an initial *control interval*. After that, the propagator error can be forecast for future instants, when control data are no longer available; consequently, it can be eventually corrected.

Therefore, a hybrid orbit propagator consists of two components: a base propagator, which generates an approximate solution, and an error forecaster, which has been previously adjusted so as to model and reproduce the base-propagator error dynamics. Two main types of forecasters have been proposed for hybrid orbit propagators: those based on statistical time-series methods [11,14,15], and those that rely on machine-learning techniques, such as neural networks [16,17]. A recent example of a hybrid orbit propagator can be found in [12], where the hybrid methodology is applied to the enhancement of the well-known orbit propagator *Simplified General Perturbations-4* (SGP4) [18,19].

In this paper we propose an extension of the hybrid methodology for orbit propagation that allows fitting a hybrid orbit propagator from others previously adjusted for nearby initial conditions. It avoids the need for both the control data and the

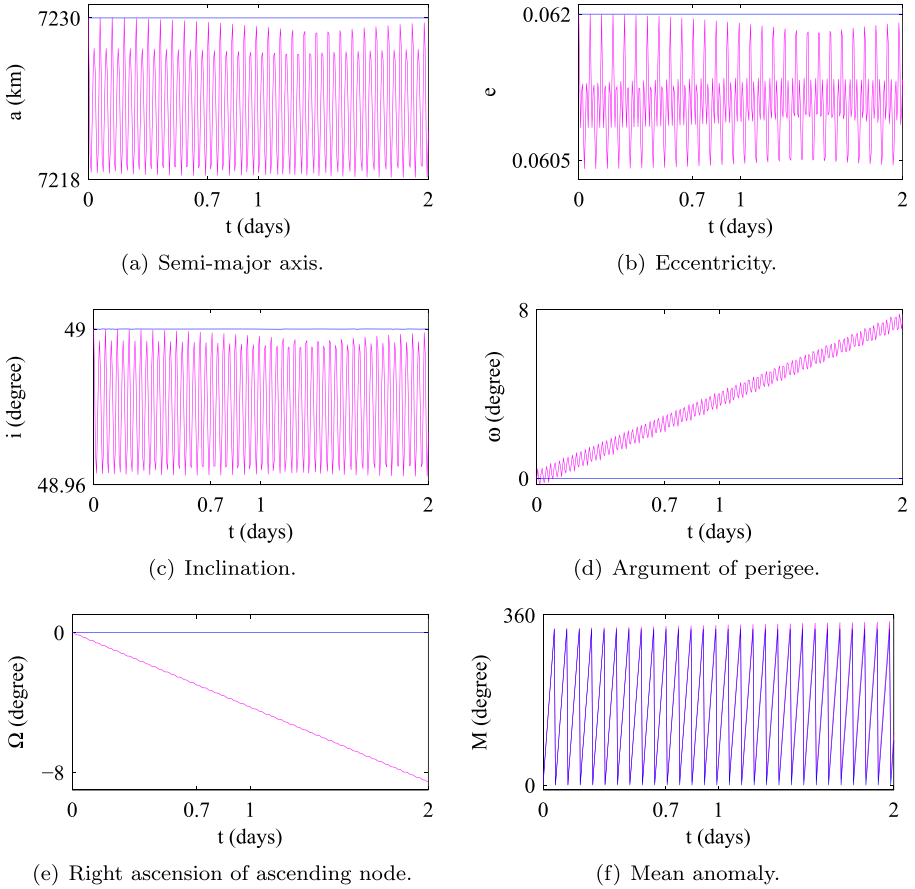

(a) Semi-major axis.

(b) Eccentricity.

(c) Inclination.

(d) Argument of perigee.

(e) Right ascension of ascending node.

(f) Mean anomaly.

Fig. 2. *Kepler problem* versus *main problem*. The evolution of all the orbital elements except the mean anomaly is constant for the *Kepler problem* (blue), whereas the J_2 perturbation introduces variations in all the orbital elements for the *main problem* (magenta).

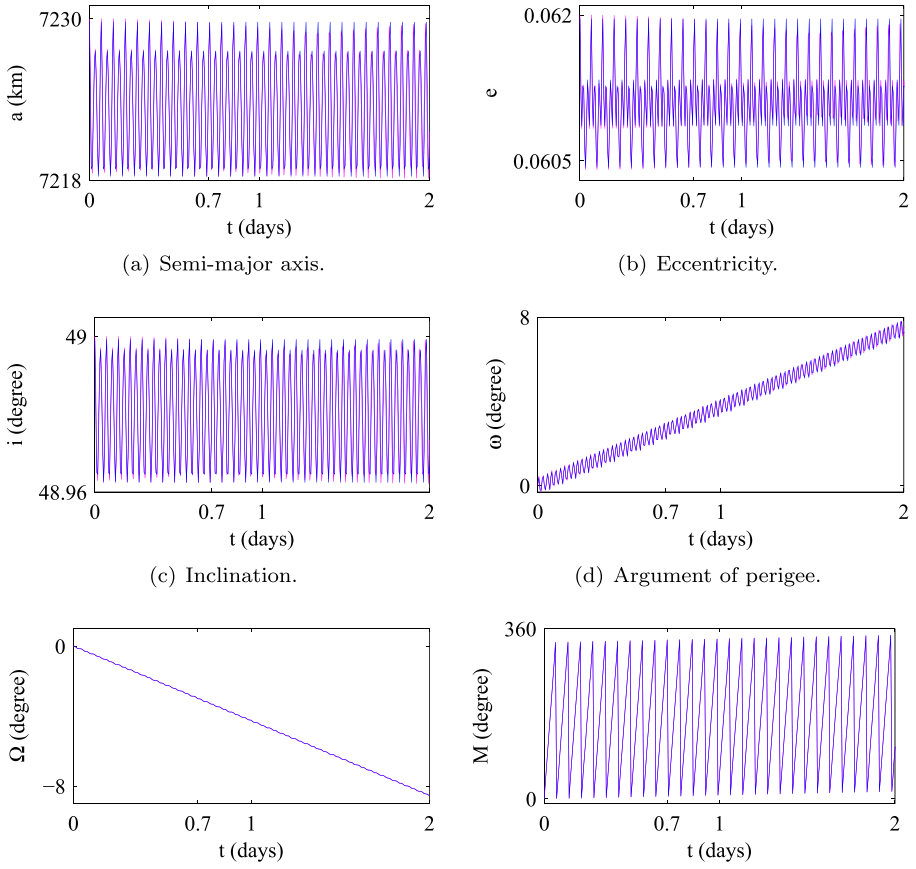

(a) Semi-major axis. (b) Eccentricity. (c) Inclination. (d) Argument of perigee. (e) Right ascension of ascending node. (f) Mean anomaly.

Fig. 3. Hybrid propagation of the *main problem*. The modeling of the J_2 *effect* by means of the forecasting component of the hybrid propagator (blue) allows complementing the base *Kepler-problem* propagator in order to approximate the *main problem* (magenta).

adjustment process, thus raising the possibility of having grids of hybrid orbit propagators prepared in advance for initial-condition regions of interest.

The outline of this paper is structured around two main sections. The first, Section 2, is focused on standard hybrid orbit propagators, whereas the second, Section 3, addresses new hybrid orbit propagators fit from standard ones. Each of these sections has two subsections. In the case of standard hybrid propagators, Section 2.1 presents a very brief overview of the forecasting method that will be used, the Holt-Winters algorithm. Then, a sample satellite is used in Section 2.2 to illustrate the application of the hybrid methodology, based on the described Holt-Winters algorithm, to the propagation of its orbit. After that, Section 3.1 starts the section devoted to fitting new hybrid propagators by developing a grid of standard hybrid propagators for a set of initial conditions surrounding those of the previously propagated satellite. Next, Section 3.2 shows how to fit new hybrid propagators for nearby initial conditions from the developed grid, and compares their accuracy to standard non-fit hybrid propagators. Finally, Section 4 summarizes the main points of the study.

Algorithm 1 Holt-Winters.

Require: s, c, h, and $\{\varepsilon_t\}_{t=1}^{T}$
Ensure: $\hat{\varepsilon}_{T+h|T}$
1: Estimate the values of $A_0, B_0, S_{-s+1}, \ldots, S_{-1}, S_0$
2: **for** $t = 1;\ t \leq T;\ t = t+1$ **do**
3: $A_t = \alpha(\varepsilon_t - S_{t-s}) + (1-\alpha)(A_{t-1} + B_{t-1})$
4: $B_t = \beta(A_t - A_{t-1}) + (1-\beta)B_{t-1}$
5: $S_t = \gamma(\varepsilon_t - A_t) + (1-\gamma)S_{t-s}$
6: $\hat{\varepsilon}_t = A_{t-1} + B_{t-1} + S_{t-s}$
7: **end for**
8: Select `error_measure` ∈ {MSE, MAE, MAPE} and express it as a function of the smoothing parameters
9: Obtain the smoothing parameters that minimize `error_measure` using the L-BFGS-B method
10: Calculate $A_T, B_T, S_{T-s+1}, \ldots, S_{T-1}, S_T$ for the optimum smoothing parameters
11: $\hat{\varepsilon}_{T+h|T} = A_T + hB_T + S_{T-s+1+h \bmod s}$
12: **return** $\hat{\varepsilon}_{T+h|T}$

2. Standard hybrid orbit propagator

2.1. Holt-Winters forecasting method

In this subsection, we briefly describe the forecasting method that will be used for the development of a standard hybrid propagator in Section 2.2.

The Holt-Winters method, originally proposed in [20], is one of the so-called *exponential smoothing* methods that can be used for time-series forecasting. It allows modeling a time series as the superposition of a linear trend and a seasonal component.

The application of the Holt-Winters method to time-series forecasting in the framework of the hybrid methodology for orbit propagation has been extensively described in [11,12,15]. Therefore, we refer any readers who can be interested in the details of the method to those references, and only include in this subsection the main concepts of the algorithm.

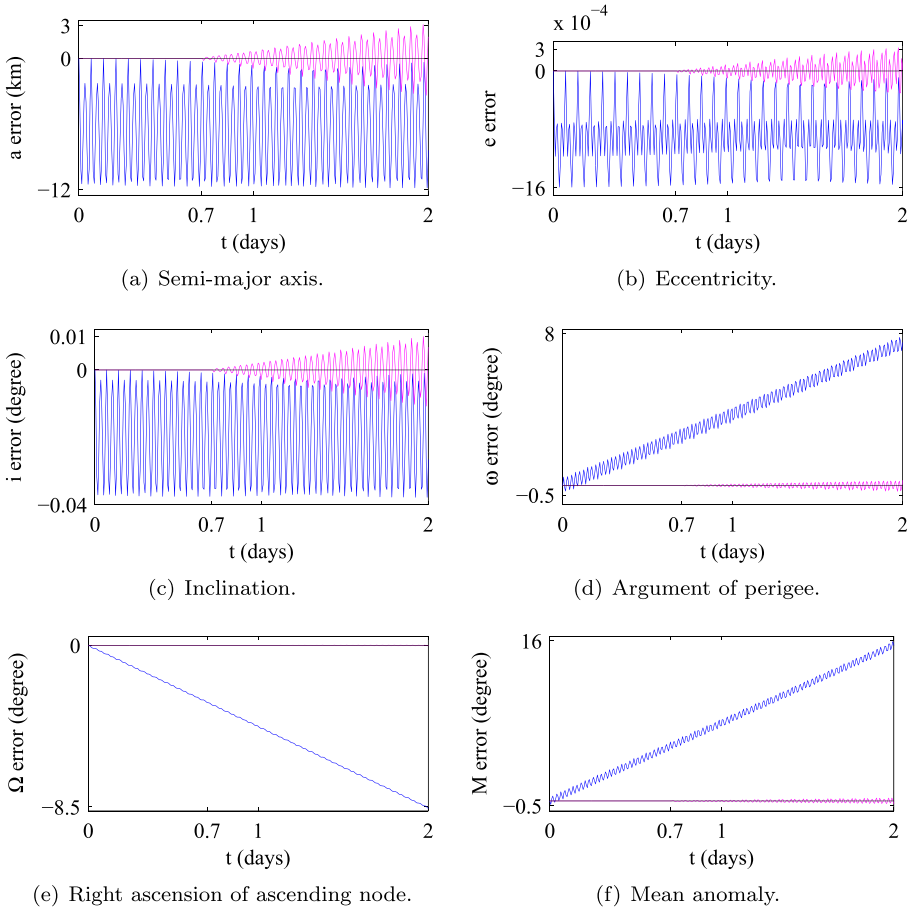

(a) Semi-major axis. (b) Eccentricity. (c) Inclination. (d) Argument of perigee. (e) Right ascension of ascending node. (f) Mean anomaly.

Fig. 4. Orbital-element errors of the base *Kepler-problem* propagation (blue) versus the complete hybrid propagation of the *main problem* (magenta) for a time span of 2 days. The hybrid propagation starts at $t = 0.7$ days, after the end of the control interval during which the forecasting component is adjusted.

The Holt-Winters method, reproduced in Algorithm 1, characterizes a time series through a set of parameters: its trend level A_t and slope B_t, and a set of points sampled from its seasonal component $(S_{t-s+1}, \ldots, S_{t-1}, S_t)$. The determination of the best-adjusted values for those parameters implies finding the optimum values of three additional *smoothing parameters,* α, β, and γ, which determine how the initially estimated values $A_0, B_0, S_{-s+1}, \ldots, S_{-1}, S_0$ are modified according to data available in the control interval. The complete process allows calculating the parameters of the best-adjusted time-series model for the last instant in the control interval (T), $A_T, B_T, S_{T-s+1}, \ldots, S_{T-1}, S_T$, from which the time-series value for any future instant h epochs ahead can be forecast as $\hat{\varepsilon}_{T+h|T} = A_T + hB_T + S_{T-s+1+h \bmod s}$.

2.2. Development of a standard hybrid orbit propagator for an illustrative satellite

In this subsection, we follow the procedure to develop a standard hybrid orbit propagator for an illustrative satellite, and present some results so as to show the enhancement that can be achieved with respect to a base orbit propagator.

Space debris and operative satellites are mainly concentrated in three different regions around the Earth: below 2000 km of altitude (Low Earth Orbits, LEO), at about 18000 km (Medium Earth Orbits, MEO), and at about 36000 km (Geostationary Earth Orbits, GEO). We choose a set of initial conditions in the LEO region that has some periodicity properties that can be maintained for a long time, thus allowing the model of the base-propagator error to be valid for medium-term propagation. This set of initial conditions is determined by a semi-major axis $a = 7230$ km, an eccentricity $e = 0.062$, and an inclination $i = 49^\circ$ (Fig. 1). In addition, these periodicity properties can also be extended to nearby orbits, therefore allowing for the medium-term validity of new error models fit from others in the vicinity. The size of these regular regions depends on the different perturbations that exert their effects in each case.

Nevertheless, space-debris objects in general do not necessarily have to be located in points in which such desirable periodicity properties exist, and therefore their behavior can change abruptly among close trajectories. A more detailed analysis of this matter would imply a qualitative description of the dynamical system in the context of the artificial satellite theory. Further details on this topic can be found in [21].

The simplest base propagator that can be considered corresponds to the *Kepler problem*, which only takes into account an ideal gravitational field that the Earth would cause if its whole mass were concentrated in its center. As Fig. 2 shows, the absence of any perturbations makes such a propagator predict a constant evolution of all the orbital elements except the mean anomaly, which varies as the satellite rotates around the Earth.

Then, we can extend the problem to include the primary perturbation that acts on LEO satellites: the gravitational effect of the Earth equatorial bulge, which is determined by the J_2 coefficient, and hence is usually referred to as the J_2 *effect*. This new problem, known as the *main problem*, is generally characterized, except for certain specific configurations, by the continuous change of the six orbital elements, as can also be seen in Fig. 2.

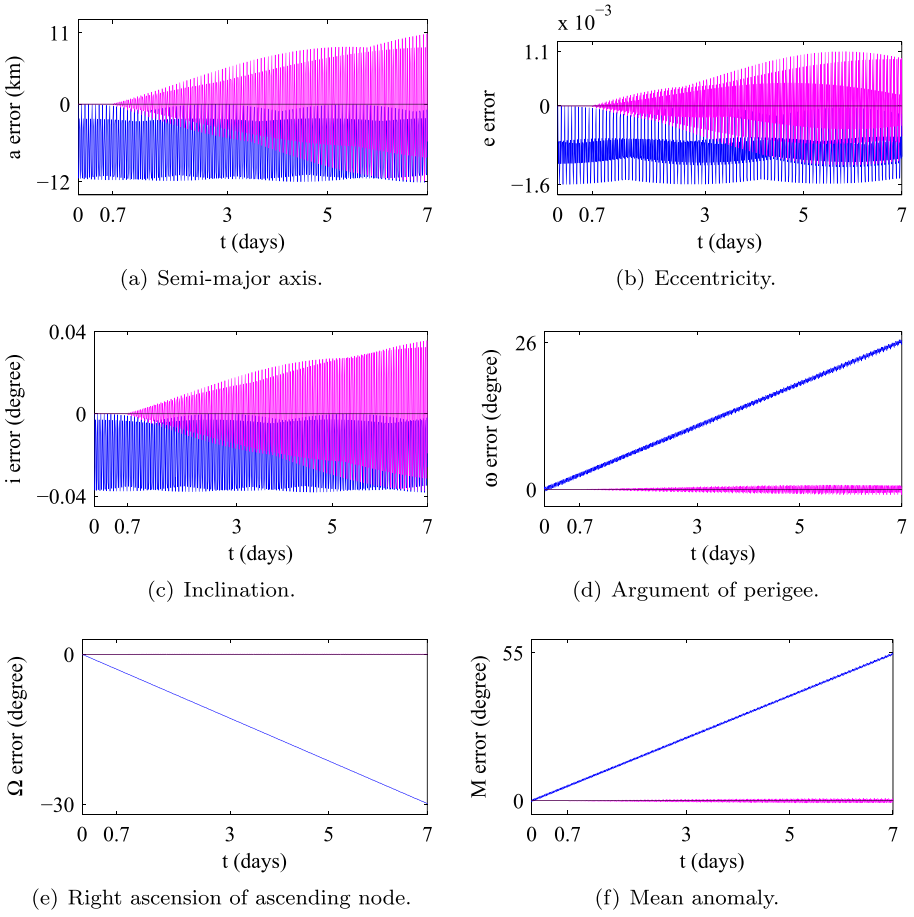

(a) Semi-major axis. (b) Eccentricity.

(c) Inclination. (d) Argument of perigee.

(e) Right ascension of ascending node. (f) Mean anomaly.

Fig. 5. Orbital-element errors of the base *Kepler-problem* propagation (blue) versus the complete hybrid propagation of the *main problem* (magenta) for a time span of 7 days. A clear improvement of the hybrid propagation in the argument of the perigee, the right ascension of the ascending node, and the mean anomaly can be observed. The hybrid propagation starts at $t = 0.7$ days, after the end of the control interval during which the forecasting component is adjusted.

Therefore, we can apply the hybrid methodology in order to develop a hybrid orbit propagator for the *main problem*, composed of a simple base propagator designed for the *Kepler problem*, and a time-series forecaster, based on the Holt-Winters algorithm described in Section 2.1, to be in charge of modeling the J_2 *effect*.

It is worth mentioning that the assessment of results will be made with respect to a set of ephemerides, which we call pseudo-observations, accurately computed by means of an 8th-order numerical Runge-Kutta integrator [22]. In addition, some of those pseudo-observations, the ones corresponding to the initial control interval, are also necessary for modeling the base-propagator error in order to adjust the Holt-Winters time-series forecaster. Nevertheless, it must be noted that real observations can also be used for this purpose in case they be available.

We consider a control interval of 10 satellite revolutions, which corresponds to approximately 0.7 days. An extensive study on the length of the control interval was conducted in [15], in which 10 revolutions was found to be optimal for the propagation of a LEO satellite during a time span of 30 days. Then we proceed with the development of a hybrid orbit propagator according to the methodology described in [11–13]. As we verified in [12], some orbital elements, such as the mean anomaly and the argument of the perigee, have a greater potential to enhance orbit propagators through the application of the hybrid methodology. Therefore, modeling only those orbital elements can be a wise strategy for developing parsimonious models. Nevertheless, in this study we model all the orbital elements, through their corresponding Delaunay action-angle variables, with the aim of maximizing accuracy.

Table 1
Maximum position error (km) after propagating the illustrative satellite.

Propagation span	Base propagator (Kepler)	Hybrid propagator (Kepler + J_2)
1 day	1204.41	2.88
2 days	2393.37	3.47
7 days	7864.46	12.39
30 days	14485.08	16.52

Finally, we propagate the orbit during the aforementioned span of 30 days.

Next, we present some results in order to illustrate the capabilities of hybrid propagators. Fig. 3 shows how the developed hybrid propagator is capable of approximating the *main problem*, which implies that its forecasting component has been able to model the J_2 *effect* quite accurately. Figs. 4–6 compare the performance of both the base *Kepler-problem* propagator and the hybrid *main-problem* propagator, in terms of the evolution of their orbital-element errors with respect to precise pseudo-observations, for different propagation spans. As can be observed, the most relevant differences lie in the argument of the perigee, the right ascension of the ascending node, and the mean anomaly, whose errors show a steady trend, called *secular component*, for the base propagator, whereas they are bounded for the hybrid propagator.

Those differences, particularly with regard to the mean-anomaly error, have a direct impact on the error of the satel-

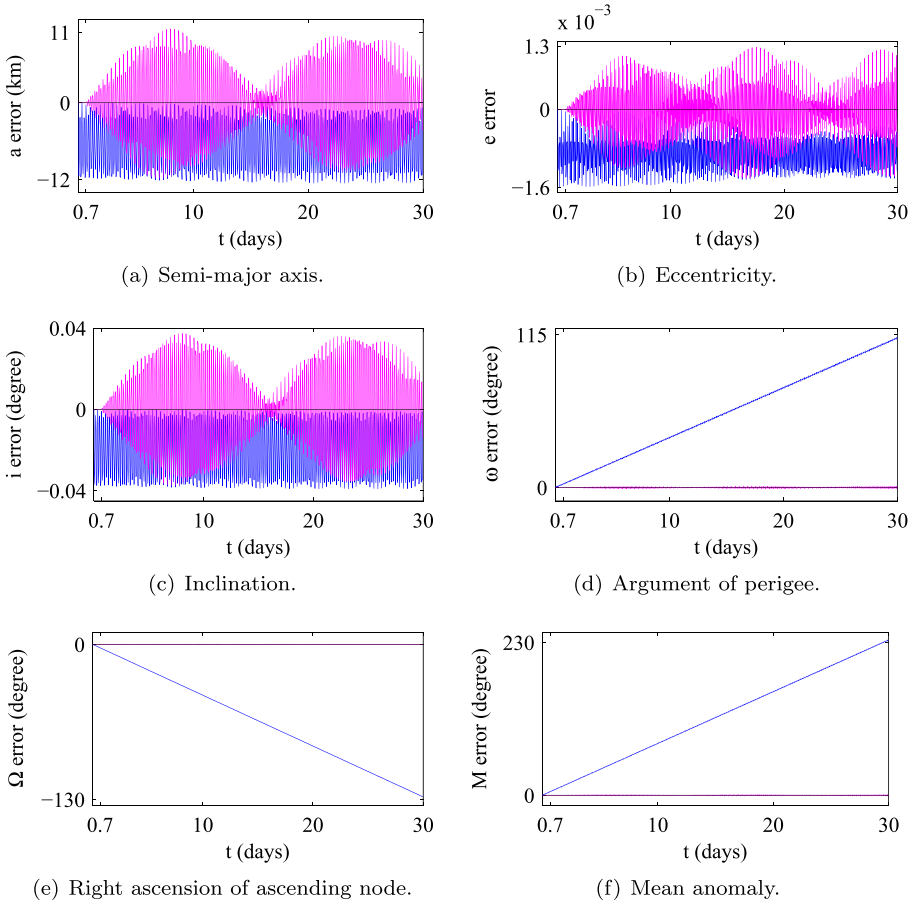

(a) Semi-major axis. (b) Eccentricity. (c) Inclination. (d) Argument of perigee. (e) Right ascension of ascending node. (f) Mean anomaly.

Fig. 6. Orbital-element errors of the base *Kepler-problem* propagation (blue) versus the complete hybrid propagation of the *main problem* (magenta) for a time span of 30 days. The marked improvement of the hybrid propagation in the argument of the perigee and right ascension of the ascending node, and especially in the mean anomaly, will have a significant effect on the overall position error of the satellite. The hybrid propagation starts at $t = 0.7$ days, after the end of the control interval during which the forecasting component is adjusted. Only 20% of the ephemerides have been plotted, without affecting the contour of the resulting figures, for the sake of clarity.

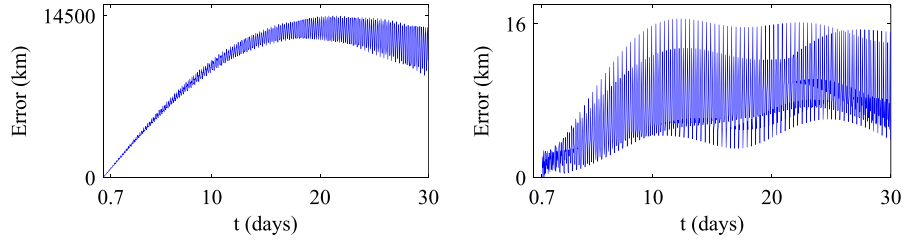

(a) Base propagation. (b) Complete hybrid propagation.

Fig. 7. Comparison between the position errors corresponding to the base *Kepler-problem* propagation and the complete hybrid propagation of the *main problem*. The modeling of the J_2 *effect* by the forecasting component of the hybrid propagator allows reducing the maximum position error from 14485.08 km to 16.52 km in a 30-day propagation. The hybrid propagation starts at $t = 0.7$ days, after the end of the control interval during which the forecasting component is adjusted. For the sake of clarity, only 20% of data have been plotted, without affecting the contour of the resulting figures.

lite predicted position, which is compared for both propagators in Fig. 7. Table 1 quantifies that position error at several time spans, showing how the modeling of the base-propagator error by the forecasting component of the hybrid propagator can lead to a dramatic reduction in the satellite position error.

Finally, Fig. 8 characterizes the hybrid-propagator position error through its three orthogonal components in the Frenet frame, with directions tangent to the orbit, *along-track error*, normal to the orbital plane, *cross-track error*, and binormal with respect to the other two components, *radial error*.

3. Fitting new hybrid orbit propagators

3.1. Surrounding grid of initial conditions

In this subsection, we develop a grid of standard hybrid orbit propagators for initial conditions around those of the illustrative satellite previously considered. From those propagators, we will fit new hybrid propagators for nearby initial conditions later, in Section 3.2. This can be an interesting practice in a context in which the illustrative satellite is located in a particularly populated region of initial conditions, which, for that reason, is especially in-

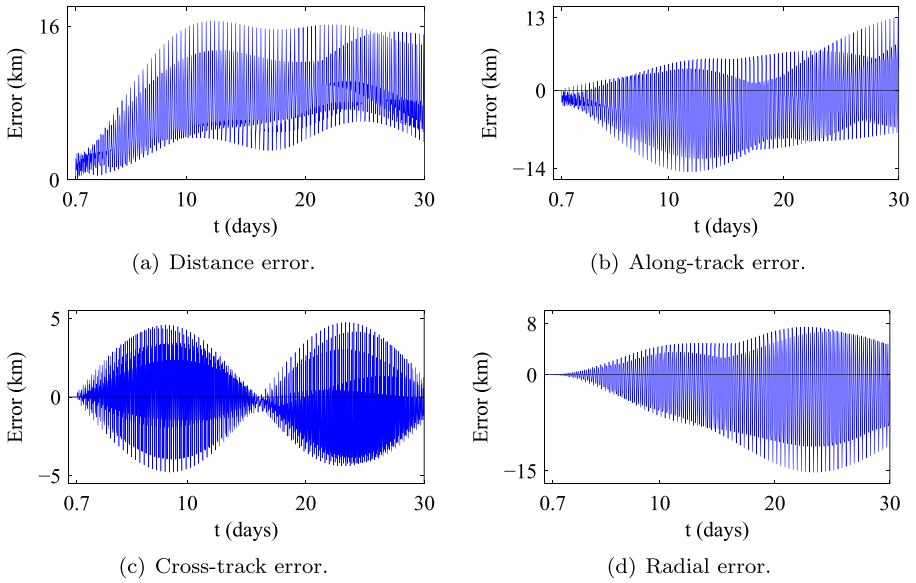

Fig. 8. Position error corresponding to the complete hybrid propagation of the *main problem*. The total distance error (a) is shown decomposed into 3 orthogonal components in the directions tangent to the orbit (b), normal to the orbital plane (c), and radial (d). The hybrid propagation starts at $t = 0.7$ days, after the end of the control interval during which the forecasting component is adjusted. For the sake of clarity, only 20% of data have been plotted, without affecting the contour of the resulting figures.

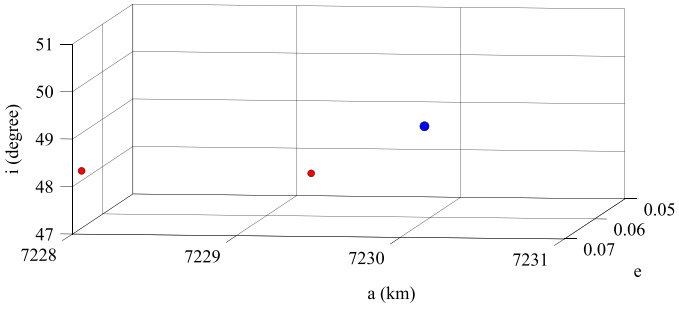

Fig. 9. New satellites to be propagated near the illustrative satellite.

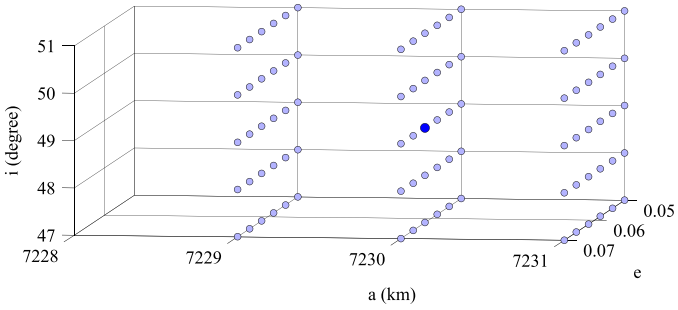

Fig. 10. Grid of initial conditions surrounding the illustrative satellite in a region of interest.

teresting from the SST point of view. In that context, the need can arise to propagate new initial conditions within that region at any time (Fig. 9). The standard procedure for developing hybrid orbit propagators for them would imply the need for control data, either in the form of real observations, which might not be available, or as pseudo-observations, which would need to be generated through relatively slow numerical integration. In addition, the Holt-Winters algorithm would have to be applied in order to adjust the forecasting component of the new hybrid propagators.

The new approach that we present in this paper is based on fitting new hybrid propagators from others previously developed for nearby initial conditions. This strategy eliminates the need for control data, and allows having sets of hybrid propagators prepared in advance for initial-condition regions of interest.

In order to implement the proposed approach, a grid of 90 initial conditions surrounding the illustrative satellite (Fig. 10) is built. In that grid, the semi-major axis is modified between 7229 km and 7231 km in 1 km steps, the eccentricity is changed between 0.05 and 0.07 in 0.004 steps, and the inclination is varied between 47° and 51° in 1° steps.

Then, hybrid orbit propagators are developed for all the initial conditions in the grid by following the standard procedure illustrated in Section 2.2. With the aim of checking the distribution of the position errors for all the hybrid propagators in the grid, box plots are generated for different propagation spans (Fig. 11). It can be observed that median values are approximately coincident with the hybrid-propagator position errors of the illustrative satellite, previously presented in Table 1. Nevertheless, the most significant feature of box plots in Fig. 11 is the little dispersion they show, with a total absence of any outliers, which makes it an appropriate scenario for fitting purposes.

The values that each of the hybrid propagators in the grid obtains for the parameters that constitute their Holt-Winters time-series forecasters, as described in Section 2.1, will be essential for the fitting process in Section 3.2. As an example, Fig. 12 depicts the trend-level parameter A, and two of the 12 parameters that have been taken to characterize the seasonal component, S_4 and S_7, for the mean-anomaly variable.

3.2. Fitting new hybrid orbit propagators for nearby initial conditions

In Section 3.1, the convenience of fitting the hybrid propagators for new initial conditions from a grid of hybrid propagators prepared in advance for a region of interest was discussed. In order to illustrate this concept, in this subsection we will develop fit hybrid propagators for the two new initial conditions shown in Fig. 13. One of them presents a semi-major axis $a = 7229.4$ km, an eccentricity $e = 0.067$, and an inclination $i = 48.2°$, and therefore lies completely within the limits of the grid. The other has the same eccentricity and inclination values, but a different semi-major axis,

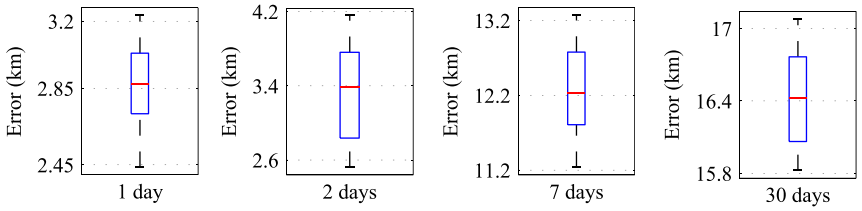

Fig. 11. Distribution of position errors corresponding to the hybrid propagation of the grid for different time spans.

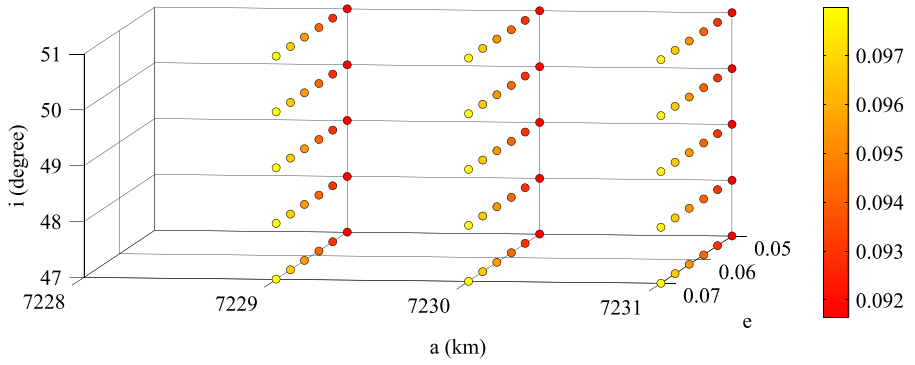

(a) Parameter A.

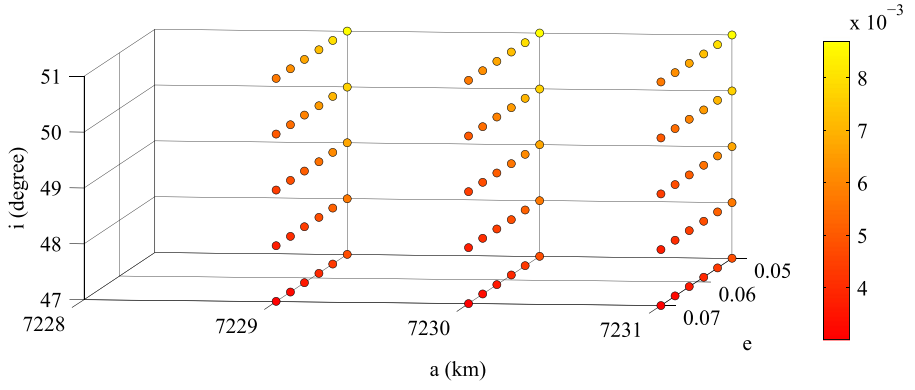

(b) Parameter S_4.

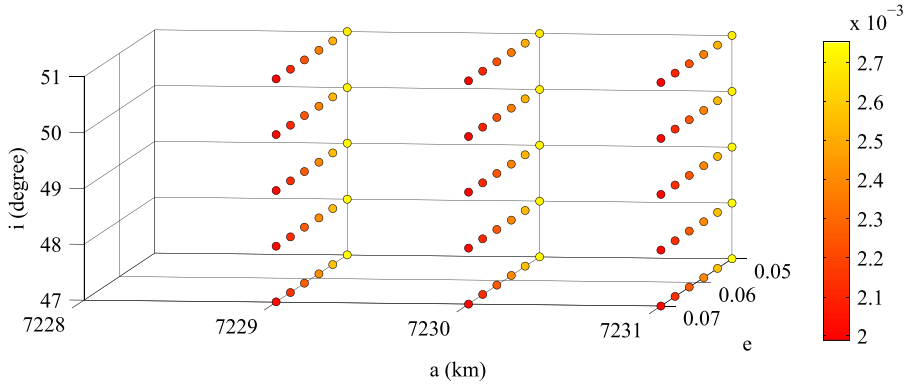

(c) Parameter S_7.

Fig. 12. Values of some sample parameters of the hybrid orbit propagators, corresponding to the mean-anomaly variable, for all the satellites in the grid.

$a = 7228$ km, which makes it lie near the grid but outside its limits.

It has been said in Section 1 that a hybrid propagator consists of a base propagator, which generates an approximate initial solution, and an error forecaster, which needs to be adjusted so as to model and reproduce the base-propagator error dynamics. The first component, that is, the base *Kepler-problem* propagator, is the same for the two initial conditions to be propagated now. However, the second component, which in this case is a Holt-Winters time-series forecaster, needs individual adjustment for each of the two satel-

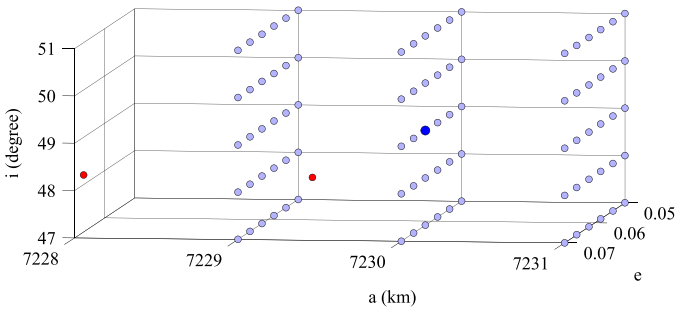

Fig. 13. The hybrid orbit propagators for the new satellites (red) will be fit from the hybrid orbit propagators prepared in advance for the set of initial conditions in the grid (light blue), which was located surrounding the illustrative satellite (dark blue) in a region of interest.

lites, due to the fact that the slight difference in their initial conditions produces a variation in their corresponding error dynamics.

As presented in Section 2.1, an adjusted Holt-Winters time-series forecaster is characterized by a set of parameters: the trend level A and slope B, and a set of samples from the seasonal component, S_i, which in this study has been taken equal to 12. The method for fitting new hybrid propagators from those in the grid, which translates into fitting new Holt-Winters time-series forecasters from the ones in the grid, will be the fitting of each of the Holt-Winters parameters from their equivalents in the grid.

First, we perform that operation by applying *Generalized Additive Models* [23,24] through their implementation in the `gam` package [25] for the R language and environment for statistical computing [26]. Fig. 14 shows the fit values for the three sample Holt-Winters parameters that were presented in Fig. 12, that is, the A,

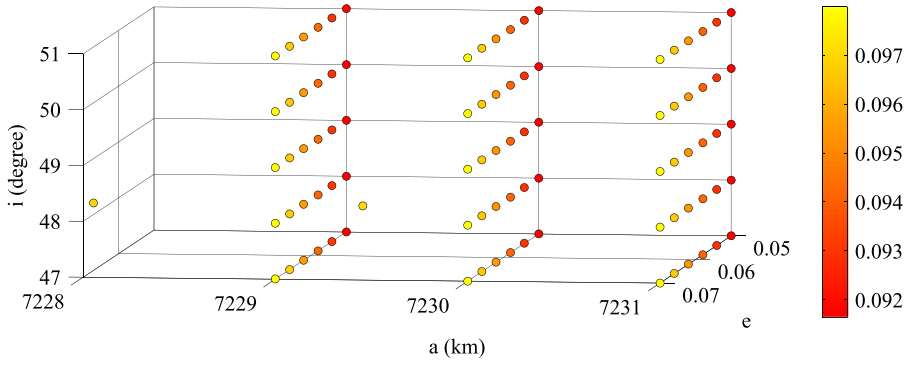

(a) Parameter A.

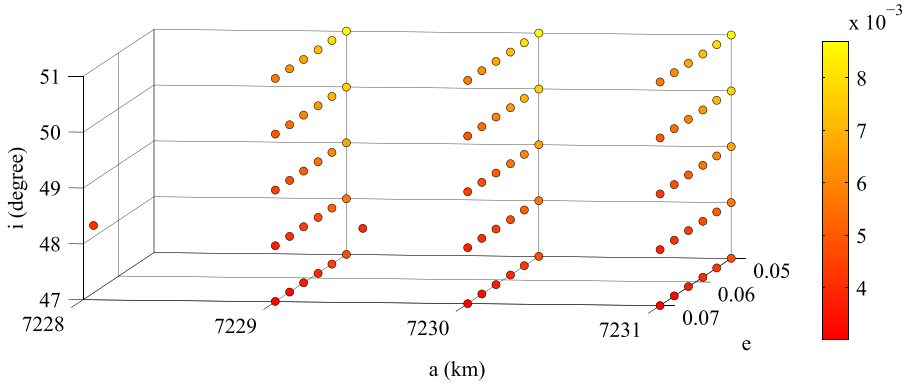

(b) Parameter S_4.

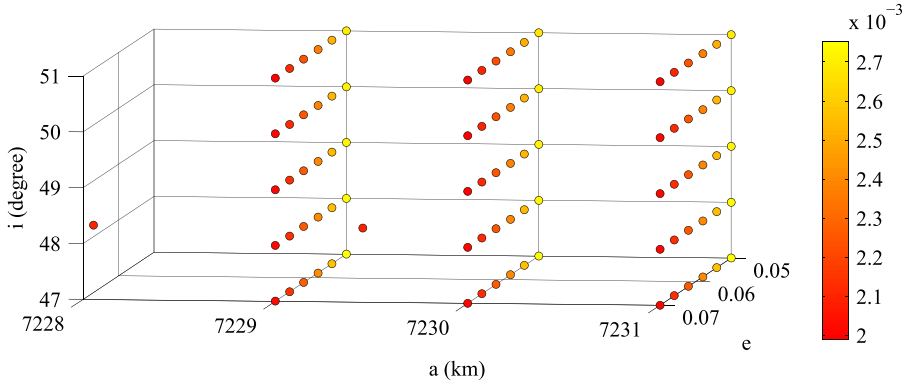

(c) Parameter S_7.

Fig. 14. Values of some sample parameters of the hybrid orbit propagators, corresponding to the mean-anomaly variable, for the new satellites. They have been fit from their equivalent parameters in all the satellites of the grid.

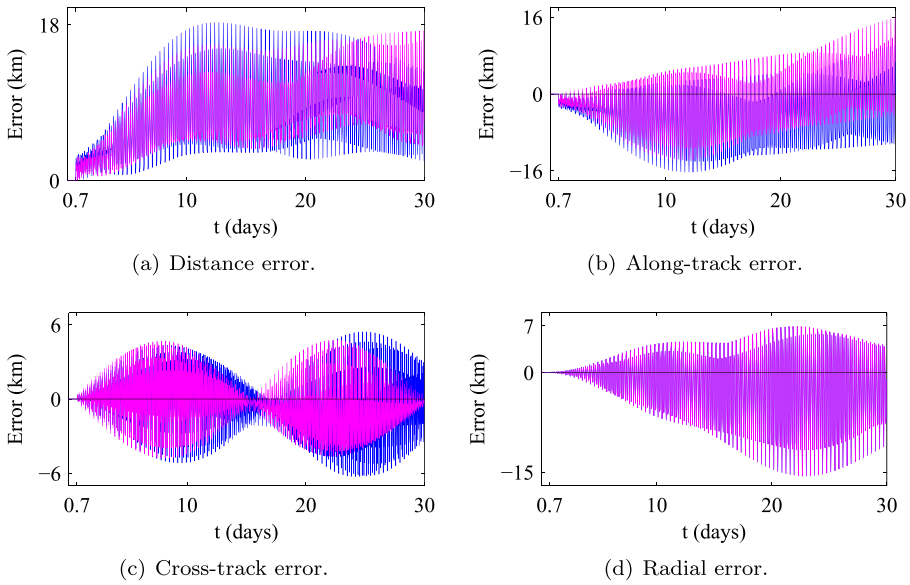

Fig. 15. Comparison between the position errors corresponding to the standard (magenta) and the fit (blue) hybrid orbit propagators for the new satellite located within the limits of the grid. The fitting process has been done by means of *Generalized Additive Models* from all the satellites in the grid. Very similar behavior can be observed for both hybrid propagators, despite the fact that no control data nor adjustment of the forecasting component is necessary for the fit one. The hybrid propagation starts at $t = 0.7$ days, after the end of the control interval during which the forecasting component of the standard hybrid propagator is adjusted. For the sake of clarity, only 20% of data have been plotted, without affecting the contour of the resulting figures.

Table 2
Maximum position error (km) after propagating the new satellite located within the limits of the grid. Columns 2–7 correspond to the base propagator (Kepler problem), the standard hybrid orbit propagator (main problem), and four fit hybrid orbit propagators (main problem) obtained through two different fitting techniques, namely *Generalized Additive Models* (gam) and *Multivariate Adaptive Regression Splines* (mars), from both a fine grid and a coarse grid of standard hybrid orbit propagators.

Time span	Base prop.	Std. HOP	Fit HOP gam, fine grid	Fit HOP gam, coarse grid	Fit HOP mars, fine grid	Fit HOP mars, coarse grid
1 day	1239.75	2.87	3.02	3.63	1.93	22.31
2 days	2462.74	3.39	4.01	5.28	2.22	44.70
7 days	8058.88	12.16	13.58	17.74	10.15	162.26
30 days	14499.62	17.34	18.29	30.25	34.61	691.53

S_4, and S_7 parameters of the mean-anomaly variable, for the two new initial conditions.

The fit hybrid propagator for the new satellite within the limits of the grid is compared in Fig. 15 with a standard hybrid propagator developed for the same case, in terms of its position error, both the total distance error and its three components in the Frenet frame. As can be observed, the behavior of both propagators is very similar, even though the fit propagator did not require any control data nor the Holt-Winters adjustment process for its development.

Table 2 quantifies, in columns 2–4, the maximum position error for different time spans when this satellite is propagated with just the base propagator, and with both the standard and the fit hybrid propagators, respectively. The comparable values obtained for these last two cases confirm their similar qualitative behavior also observed in Fig. 15.

Then, with the aim of testing the effect of the grid density, we develop a new hybrid propagator for the same satellite from a coarser grid, composed only of the eight satellites in its vertices. The maximum position errors displayed in column 5 of Table 2 show that, as could be presumed, the accuracy is reduced with respect to the results obtained in column 4 from a finer grid.

Next, we try another fitting technique, *Multivariate Adaptive Regression Splines*, which builds regression models by using the techniques described in [27,28]. For that purpose, we use the `earth` package [29] in the same R environment. The last two columns in Table 2 display the maximum position errors obtained when the fitting process is performed from both the complete grid and the eight-vertex coarser grid. As can be observed, this fitting technique can lead to very good results in the short term when a fine grid is used, although accuracy deteriorates with time faster than in the case of *Generalized Additive Models*. In fact, after a 30-day propagation, the error corresponding to the application of *Multivariate Adaptive Regression Splines* to the fine grid is comparable to the error obtained when *Generalized Additive Models* are applied to the coarse grid. However, the use of *Multivariate Adaptive Regression Splines* with the coarse grid produces markedly worse results.

Finally, the same process is followed for the other new satellite, the one located outside the limits of the grid. Fig. 16 depicts the evolution of the position error for two hybrid propagators, the standard one and the one fit from the complete grid through *Generalized Additive Models*. In addition, similar to Table 2, Table 3 compares the maximum position errors for the base propagator and for five hybrid propagators: the standard one and the four that have been fit both through the two considered techniques and from the same two grids, the fine and the coarse. In general, results are worse than those obtained for the previously analyzed new satellite, the one located within the limits of the grid, which

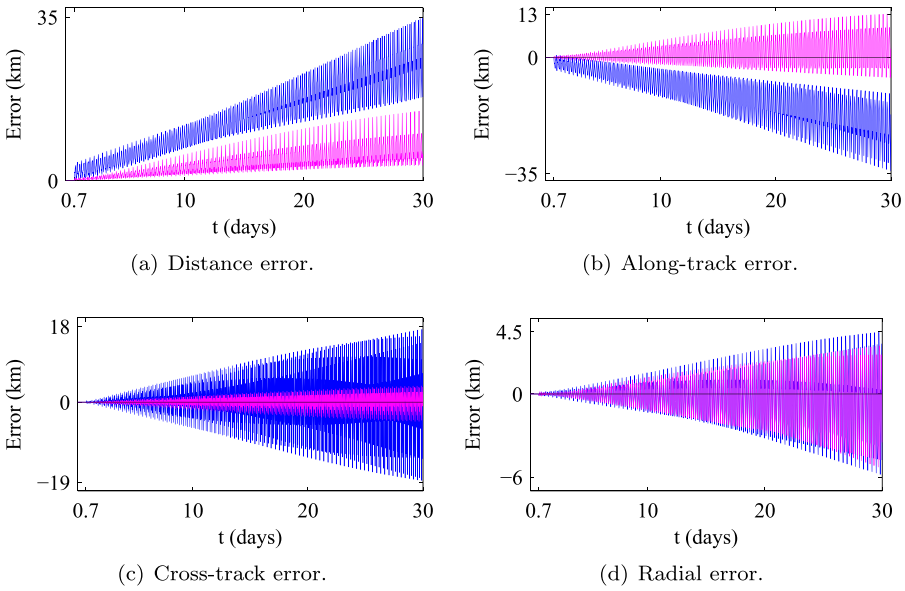

(a) Distance error. (b) Along-track error.

(c) Cross-track error. (d) Radial error.

Fig. 16. Comparison between the position errors corresponding to the standard (magenta) and the fit (blue) hybrid orbit propagators for the new satellite located outside the limits of the grid. That condition causes the fit hybrid propagator to behave slightly worse than the standard one. The fitting process has been done by means of *Generalized Additive Models* from all the satellites in the grid. The hybrid propagation starts at $t = 0.7$ days, after the end of the control interval during which the forecasting component of the standard hybrid propagator is adjusted. For the sake of clarity, only 20% of data have been plotted, without affecting the contour of the resulting figures.

Table 3
Maximum position error (km) after propagating the new satellite located outside the limits of the grid. Columns 2–7 correspond to the base propagator (Kepler problem), the standard hybrid orbit propagator (main problem), and four fit hybrid orbit propagators (main problem) obtained through two different fitting techniques, namely *Generalized Additive Models* (gam) and *Multivariate Adaptive Regression Splines* (mars), from both a fine grid and a coarse grid of standard hybrid orbit propagators.

Time span	Base prop.	Std. HOP	Fit HOP gam, fine grid	Fit HOP gam, coarse grid	Fit HOP mars, fine grid	Fit HOP mars, coarse grid
1 day	1240.22	0.56	3.96	6.40	4.13	22.42
2 days	2465.05	0.82	4.89	9.52	5.68	43.81
7 days	8143.63	3.72	9.39	25.17	13.36	151.88
30 days	14506.80	14.95	34.96	100.34	51.23	626.64

is something intuitive. Now, the best fit hybrid propagator, which is again the one based on *Generalized Additive Models* and the fine grid, behaves slightly worse than the standard hybrid propagator. In addition, the effect of a coarser grid is more noticeable. The hybrid propagator fit from the fine grid through *Multivariate Adaptive Regression Splines* continues to achieve good results in the short term, but not better than the equivalent propagator developed by means of *Generalized Additive Models*. Finally, the fitting technique *Multivariate Adaptive Regression Splines* again shows its main weakness when it is applied to the coarse grid.

4. Conclusion

We have illustrated how the hybrid methodology for orbit propagation can help improve the precision of any propagator by applying it to a base *Kepler-problem* propagator in order to develop a hybrid *main-problem* propagator. We have verified that a time-series forecaster based on the Holt-Winters exponential-smoothing method is able to model the J_2 *effect*.

Nevertheless, since developing a hybrid orbit propagator requires some initial control data, in the form of either real observations or accurately computed pseudo-observations, as well as a tuning process for the forecasting component, the opportunity arises to seek some method for having work done in advance so that new hybrid propagators can be developed very quickly as soon as they are needed.

With this aim in mind, a grid of hybrid propagators can be developed for a set of initial conditions in a region of interest, in which the future need to propagate any satellites can arise. Then, preparing new hybrid propagators for nearby initial conditions can be done by fitting their Holt-Winters time-series-forecaster parameters from their equivalents in the grid, for which no control data nor tuning process are necessary.

It has been checked that, as could be expected, better results can be achieved when the initial conditions of the new satellite to be propagated are closer to the initial conditions in the grid. Coherently, it has also been verified that the higher the density of the grid, the more precise the results that can be obtained. When the new satellite lies within the limits of the grid, a fit hybrid propagator can be comparable to a standard hybrid propagator in terms of accuracy.

Two fitting techniques, namely *Generalized Additive Models* and *Multivariate Adaptive Regression Splines*, have been compared. The former has proven to be more reliable, although the latter can lead to better results in the short term when it is applied to a dense grid. Nevertheless, the use of *Multivariate Adaptive Regression Splines* with a coarse grid has proven to be very inaccurate.

Future work will address the applicability of this technique when other non-conservative perturbations are taken into account, as well as in other orbital regimes. Likewise, the effect of more complex perturbation models will also be assessed.

Acknowledgments

This work has been funded by the Spanish State Research Agency and the European Regional Development Fund under Project ESP2016-76585-R (AEI/ERDF, EU). Support from the European Space Agency through Project Ariadna Hybrid Propagation (ESA Contract No. 4000118548/16/NL/LF/as) is also acknowledged. The authors would like to thank two anonymous reviewers for their valuable suggestions.

References

[1] H. Kinoshita, H. Nakai, Numerical integration methods in dynamical Astronomy, Celest. Mech. 45 (1) (1989) 231–244, doi:10.1007/BF01229006.
[2] A.C. Long, J.O. Cappellari, C.E. Velez, A.J. Fuchs, Goddard Trajectory Determination System (GTDS) mathematical theory (revision 1), Technical Report CSC/TR-89/6001, Computer Sciences Corporation, 1989.
[3] D. Brouwer, Solution of the problem of artificial satellite theory without drag, Astron. J. 64 (1274) (1959) 378–397, doi:10.1086/107958.
[4] Y. Kozai, Second-order solution of artificial satellite theory without air drag, Astron. J. 67 (7) (1962) 446–461, doi:10.1086/108753.
[5] R.H. Lyddane, Small eccentricities or inclinations in the Brouwer theory of the artificial satellite, Astron. J. 68 (8) (1963) 555–558, doi:10.1086/109179.
[6] K. Aksnes, A second-order artificial satellite theory based on an intermediate orbit, Astron. J. 75 (9) (1970) 1066–1076, doi:10.1086/111061.
[7] H. Kinoshita, Third-order Solution of an Artificial-satellite Theory, Special Report no. 379, Smithsonian Astrophysical Observatory, Cambridge, MA, USA, 1977.
[8] J.J.F. Liu, R.L. Alford, Semianalytic theory for a close-Earth artificial satellite, J. Guid. Control Dyn. 3 (4) (1980) 304–311, doi:10.2514/3.55994.
[9] J.G. Neelon Jr., P.J. Cefola, R.J. Proulx, Current development of the Draper Semi-analytical Satellite Theory standalone orbit propagator package, Adv. Astronaut. Sci. 97 (1998) 2037–2052. Paper AAS 97–731
[10] P.J. Cefola, D. Phillion, K.S. Kim, Improving access to the semi-analytical satellite theory, Adv. Astronaut. Sci. 135 (2010) 46. Paper AAS 09–341
[11] J.F. San-Juan, M. San-Martín, I. Pérez, R. López, Hybrid perturbation methods based on statistical time series models, Adv. Space Res. 57 (8) (2016) 1641–1651. Advances in Asteroid and Space Debris Science and Technology - Part 2. doi: 10.1016/j.asr.2015.05.025.
[12] J.F. San-Juan, I. Pérez, M. San-Martín, E.P. Vergara, Hybrid SGP4 orbit propagator, Acta Astronaut. 137 (2017) 254–260, doi:10.1016/j.actaastro.2017.04.015.
[13] I. Pérez, M. San-Martín, R. López, E.P. Vergara, A. Wittig, J.F. San-Juan, Forecasting satellite trajectories by interpolating hybrid orbit propagators, Lect. Notes Comput. Sci. 10334 (2017) 650–661, doi:10.1007/978-3-319-59650-1_55.
[14] J.F. San-Juan, M. San-Martín, I. Pérez, An economic hybrid J_2 analytical orbit propagator program based on SARIMA models, Math. Probl. Eng. 2012 (2012) 15. Article ID 207381. doi: 10.1155/2012/207381.
[15] M. San-Martín, Métodos de propagación híbridos aplicados al problema del satélite artificial. Técnicas de suavizado exponencial, Ph.D. thesis, University of La Rioja, Spain, 2014.
[16] I. Pérez, J.F. San-Juan, M. San-Martín, L.M. López-Ochoa, Application of computational intelligence in order to develop hybrid orbit propagation methods, Math. Probl. Eng. 2013 (2013) 11. Article ID 631628. doi: 10.1155/2013/631628.
[17] I. Pérez, Aplicación de técnicas estadísticas y de inteligencia computacional al problema de la propagación de órbitas, Ph.D. thesis, University of La Rioja, Spain, 2015.
[18] F.R. Hoots, R.L. Roehrich, Models for propagation of the NORAD element sets, Spacetrack Report #3, U.S. Air Force Aerospace Defense Command, Colorado Springs, CO, USA, 1980.
[19] D.A. Vallado, P. Crawford, R. Hujsak, T.S. Kelso, Revisiting spacetrack report #3, in: Proceedings 2006 AIAA/AAS Astrodynamics Specialist Conference and Exhibit, 3, American Institute of Aeronautics and Astronautics, Keystone, CO, USA, 2006, pp. 1984–2071. Paper AIAA 2006–6753. doi: 10.2514/6.2006-6753.
[20] P.R. Winters, Forecasting sales by exponentially weighted moving averages, Manag. Sci. 6 (3) (1960) 324–342, doi:10.1287/mnsc.6.3.324.
[21] S.L. Coffey, A. Deprit, E. Deprit, Frozen orbits for satellites close to an Earth-like planet, Celest. Mech. Dyn. Astron. 59 (1) (1994) 37–72, doi:10.1007/BF00691970.
[22] J.R. Dormand, P.J. Prince, Practical Runge–Kutta processes, SIAM J. Sci. Stat. Comput. 10 (5) (1989) 977–989, doi:10.1137/0910057.
[23] T.J. Hastie, R.J. Tibshirani, Generalized Additive Models, Monographs on Statistics and Applied Probability, 43, Chapman & Hall, London, UK, 1990.
[24] T.J. Hastie, Generalized additive models, in: J.M. Chambers, T.J. Hastie (Eds.), Statistical Models in S, Computer Science Series, Chapman & Hall, 1991.
[25] T. Hastie, GAM: Generalized Additive Models, R Foundation for Statistical Computing, 2018. R package version 1.15.
[26] R Core Team, R: A Language and Environment for Statistical Computing, R Foundation for Statistical Computing, Vienna, Austria, 2017.
[27] J.H. Friedman, Multivariate Adaptive Regression Splines (with discussion), Ann. Stat. 19 (1) (1991) 1–141, doi:10.1214/aos/1176347963.
[28] J.H. Friedman, Fast MARS, Technical Report 110, Stanford University, Department of Statistics, Stanford, CA, USA, 1993.
[29] S. Milborrow, derived from mda:mars by Trevor Hastie and Rob Tibshirani, earth: Multivariate Adaptive Regression Splines, R Foundation for Statistical Computing, 2018. R package version 4.6.2.

Iván Pérez received a B.Sc. in Electronics Engineering, a M.Sc. in Industrial Engineering, and a Ph.D. in Electrical Engineering, Mathematics and Computer Science from the University of La Rioja (UR), Spain. He has been an Associate Professor at UR since 1998, where he is a member of the Scientific Computing Group (GRUCACI). His main field of research is focused on the application of machine learning to the space domain, in particular to the propagation of satellite orbits through hybrid methodologies. He has participated in research contracts funded by the Centre National d'Études Spatiales (CNES) and the European Space Agency (ESA).

Montserrat San-Martín received a M.Sc. in Mathematics from the University of Zaragoza, Spain, and a Ph.D. in Electrical Engineering, Mathematics and Computer Science from the University of La Rioja (UR), Spain. She worked as an Associate Professor at UR between 1988 and 2014. Currently she is an Associate Professor at the Department of Statistics and Operations Research at the University of Granada, Spain, a member of the Scientific Computing Group (GRUCACI), and an Associate Researcher at the Center for Biomedical Research of La Rioja (CIBIR). Her main research interest is focused on statistical analysis applied to Astrodynamics and Health Sciences.

Rosario López received a Ph.D. in Electrical Engineering, Mathematics and Computer Science from the University of La Rioja (UR), Spain. She started lecturing on Computer Science as an Assistant Professor at the UR School of Nursing in 2013. She has worked on big-data applications for HPC as a Bioinformatician Researcher at the Center for Biomedical Research of La Rioja. She possesses proven expertise in developing scientific computing software provided with web interface to allow access through the Internet. She has participated in several research contracts funded by the Centre National d'Études Spatiales, the European Space Agency, and the Spanish government.

Eliseo P. Vergara (Ph.D.) was born in Spain in 1967. He graduated as an Industrial Engineer at the University of Oviedo (Spain) and received a Ph.D. from the same University in 2000. He is an Associate Professor at the University of La Rioja (Spain). His research activities focus on the use of data mining and deep learning methods to solve real problems in several fields, in particular in the propagation of satellite orbits. He has participated in several research contracts funded by the European Space Agency (ESA) and the Spanish government.

Alexander Wittig is a lecturer in astronautics at the University of Southampton, UK. He received an MS in Physics followed by a dual-degree Ph.D. in Mathematics and Physics from Michigan State University in 2007 and 2011 respectively. He then returned to Europe where he worked as a Marie-Curie experienced researcher at Politecnico di Milano followed by a research fellowship at the European Space Agency's Advanced Concepts Team. He started his current position as lecturer in 2017.

Juan Félix San-Juan is a senior researcher in the field of Scientific Computing applied to real problems, mainly in the space domain, at University of La Rioja (UR), where he founded the Scientific Computing Group. He received M.Sc. and Ph.D. degrees in Mathematics from University of Zaragoza (UZ) in 1990 and 1996, respectively. He has been an Associate Professor at UZ and UR since 1992. He has published more than 100 articles in scientific journals, and has participated in R&D projects funded by space agencies and European bodies with a total budget of 1.3 M€ in the last 5 years.